J|A|C|S
ARTICLES
Published on Web 01/05/2002

Spontaneous Resolution Induced by Self-Organization of Chiral Self-Complementary Cobalt(III) Complexes with Achiral Tripod-Type Ligands Containing Three Imidazole Groups

Ikuko Katsuki,[†] Yuri Motoda,[†] Yukinari Sunatsuki,[†] Naohide Matsumoto,*[,†] Toshio Nakashima,[‡] and Masaaki Kojima[§]

Contribution from the Department of Chemistry, Faculty of Science, Kumamoto University, Kurokami 2-39-1, Kumamoto 860-8555, Japan, Department of Chemistry, Faculty of Education and Welfare Science, Oita University, Dan-noharu 700, Oita 870-1192, Japan, and Department of Chemistry, Faculty of Science, Okayama University, Tsushima-naka 3-1-1, Okayama 700-8530, Japan

Received October 19, 2001

Abstract: The progression from synthetically achiral ligand and metal ion, to isolated chiral metal complex, to homochiral two-dimensional (2D) assembly layer, and finally to conglomerate is presented. The cobalt(III) complexes of achiral tripod-type ligands involving three imidazole groups with the chemical formulas $[Co(H_3L^6)](ClO_4)_3 \cdot H_2O$ (**6**) and $[Co(H_3L^7)](ClO_4)_3 \cdot 0.5H_2O$ (**7**) were synthesized, where H_3L^6 = tris[2-(((imidazol-4-yl)methylidene)amino)ethyl]amine and H_3L^7 = tris[2-(((2-methylimidazol-4-yl)methylidene)-amino)ethyl]amine. Each complex induces the chirality of clockwise (*C*) and anticlockwise (*A*) enantiomers due to the screw coordination arrangement of the achiral tripod-type ligand around the Co(III) ion. The fully protonated (**6**, **7**), the formally hemi-deprotonated (**6′**, **7′**), and the fully deprotonated (**6″**, **7″**) complexes were obtained as good quality crystals by adjusting the pH of the solutions. The crystal structures were determined by single-crystal X-ray analyses. There is no intermolecular network structure in the fully protonated complexes (**6**, **7**). The fully deprotonated complexes (**6″**, **7″**) form a hydrogen-bonded network structure, in which the *C* and *A* enantiomers coexist and are connected through a water molecule. The formally hemi-deprotonated species $[Co(H_{1.5}L^{6\text{ or }7})]^{1.5+}$, which functions as a self-complementary chiral building block, generates equal numbers of protonated and deprotonated molecules by an acid−base reaction to form an extended 2D homochiral layer structure consisting of a hexanuclear structure with a trigonal void as a unit. The 2D structure arises from the intermolecular imidazole−imidazolate hydrogen bonds between $[Co(H_3L^{6\text{ or }7})]^{3+}$ and $[Co(L^{6\text{ or }7})]^0$, in which adjacent molecules with the same chirality are arrayed in an up-and-down fashion. In the crystal lattices of the perchlorate salts (**6′**, **7′**), the perchlorate ions are located in the cavity, and the homochiral layer consisting of *C* enantiomers and the adjacent layer consisting of *A* enantiomers are stacked alternately to give an achiral crystal. The chloride salt of the hemi-deprotonated complex $[Co(H_{1.5}L^6)]Cl_{1.5} \cdot 4H_2O$ (**6a′**) is found to be a conglomerate, in which the chloride ions are positioned in the intermediate region of the double layer, and layers with the same chirality are well stacked by adopting the up-and-down layer's shape to generate channels, and so form a chiral crystal. The circular dichroism (CD) spectrum of **6a′** showed a positive peak and a negative peak at 480 and 350 nm, respectively, and the spectrum of another crystal showed an enantiomeric CD pattern, providing further evidence of spontaneous resolution on crystallization.

Introduction

Since the historic discovery of spontaneous resolution in ammonium sodium tartrate by Louis Pasteur,[1] chirality has been an important topic in chemistry, pharmacy, and living organisms.[2−4] Chirality is expressed at both the molecular and supramolecular levels.[5−9] The initial progress in chirality was in the generation of molecular chirality from the reaction of achiral components, which developed into assembling isolated chiral molecules.

[†] Kumamoto University.
[‡] Oita University.
[§] Okayama University.

(1) Pasteur, L. *Ann. Chim. Phys.* **1848**, *24*, 442−459.
(2) (a) Noyori, R. *Asymmetric Catalysis in Organic Synthesis*; John Wiley & Sons: New York, 1994. (b) Palyi, G.; Zucchi, C.; Caglitoti, L. *Advances in Biochirality*; Elsevier: Oxford, 1999.
(3) Prins, L. J.; Huskens, J.; Jong, F.; Timmerman, P.; Reinhoudt, D. N. *Nature* **1999**, *398*, 498−502.
(4) Soo, J.; Whang, D. Lee, H.; Jun, S. I.; Oh, J.; Jeon, Y. J.; Kim, K. *Nature* **2000**, *404*, 982−986.
(5) Lehn, J.-M. *Supramolecular Chemistry, Concepts and Perspectives*; VCH: Weinheim, 1995.
(6) Geib, S. J.; Vicent, C.; Fan, E.; Hamilton, A. D. *Angew. Chem., Int. Ed. Engl.* **1993**, *32*, 119−121.
(7) Woods, C. R.; Benaglia, M.; Cozzi, F.; Siegel, J. S. *Angew. Chem., Int. Ed. Engl.* **1996**, *35*, 1830−1833.
(8) (a) Tadokoro, M.; Isobe, K.; Uekusa, H.; Ohashi, Y.; Toyota, J.; Tashiro, K.; Nakasuji, K. *Angew. Chem., Int. Ed.* **1999**, *38*, 95−98. (b) Tadokoro, M.; Nakasuji, K. *Coord. Chem. Rev.* **2000**, *198*, 205−218.
(9) (a) Konno, T.; Nagashio, T.; Okamoto, K.; Hidaka, J. *Inorg. Chem.* **1992**, *31*, 1160−1165. (b) Konno, T.; Chikamoto, Y.; Okamoto, K.; Yamaguchi, T.; Ito, T.; Hirotsu, M. *Angew. Chem., Int. Ed.* **2000**, *39*, 4098−4101.

10.1021/ja0123960 CCC: $22.00

When a chiral molecule aggregates and crystallizes, it can form either (1) a racemic compound, (2) a conglomerate (racemic mixture), or (3) a racemic solid solution.[10] Jacques et al. reported that, statistically, between 5 and 10% of all racemates form conglomerate crystals,[11] indicating that homochiral interaction in the formation of crystalline racemates is usually weaker than heterochiral interaction.[12] Although the formation of conglomerates vs racemic compounds is determined by the laws of physics under specific conditions, these laws are not yet fully understood, and therefore the formation of conglomerates cannot be predicted a priori.[13] If enantioselective homochiral molecular discrimination arising from substantially strong, selective, and directional interactions, such as a coordination bond[14] or a hydrogen bond,[15] can be extended from two adjacent molecules to one-dimensional (1D), 2D, and 3D systems, then a conglomerate exhibiting 3D intermolecular homochiral interaction, and hence showing spontaneous resolution on crystallization, would be achieved.[16] The question to be answered in the most essential and difficult step toward this purpose is, "How can we design a particular molecule exhibiting an intermolecular homochiral interaction and a multidimensional extended structure?"

To realize the above-mentioned synthetic strategy, we have focused on metal complexes with polydentate ligands involving imidazole groups,[17,18] because a metal complex with an imidazole group can be a versatile self-complementary building component by the formation of coordination and hydrogen bonds.[19−23] Previously, we have reported the chiral self-complementary copper(II) complexes $[Cu(H_2L^n)](ClO_4)_2$ (n = 1−5) with achiral pentadentate strand-type ligands involving two imidazole groups per molecule **1**−**5** (Figure 1).[22] These complexes become either *C* (clockwise) or *A* (anticlockwise) enantiomers, due to the spiral coordination arrangement of their achiral ligands. The mono-deprotonated complex $[Cu(HL^n)]ClO_4$ (n = 1−5) has one imidazole and one imidazolate moiety per molecule, **1′**−**5′**, which functions as a chiral self-complementary building component, and may possibly aggregate into heterochiral (...*CACA*...) and homochiral (...*CCCC*... and ...*AAAA*...) 1D zigzag chains, due to the hydrogen bond between the imidazole and imidazolate groups of adjacent units, as shown schematically in Figure 1. Compounds **1′**−**3′**, with the less bulky substituent at the 2-position of the imidazole moiety, yielded either a ...*CCCC*... or an ...*AAAA*... isotactic 1D zigzag chain, while compounds **4′** and **5′** with the bulky substituent yielded ...*CACA*... syndiotactic 1D zigzag chains. As in the case of compounds **1′**−**3′**, the homochiral 1D chain can be easily produced, but the homochiral ...*CCCC*... and ...*AAAA*... chains are arrayed alternately to give an achiral crystal.

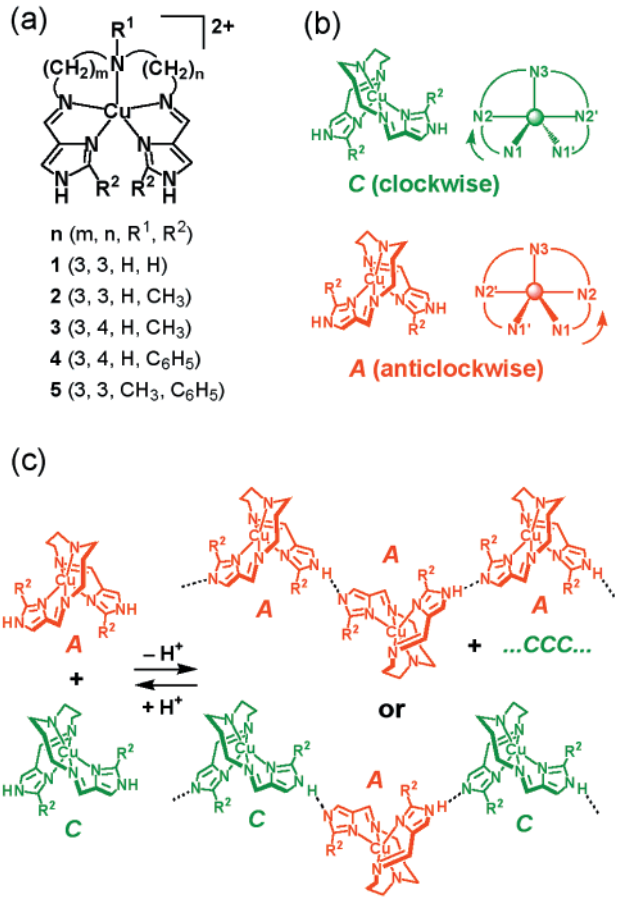

Figure 1. (a) Molecular structures of copper(II) complexes **1**−**5** with pentadentate ligands, where **n**(m, n, R^1, R^2) = **1**(3, 3, H, H); **2**(3, 3, H, CH_3); **3**(3, 4, H, CH_3); **4**(3, 4, H, C_6H_5); **5**(3, 3, CH_3, C_6H_5). (b) Structures of *C* (clockwise, green) and *A* (anticlockwise, red) enantiomers. (c) Two possible 1D structures of the mono-deprotonated complex formed by hydrogen bonds between two adjacent enantiomers, homochiral (upper: **1**, **2**, **3**) and heterochiral (lower: **4**, **5**) 1D zigzag chains.

To increase the dimensionality from 1D to 2D, we have designed cobalt(III) complexes with achiral tripod-type ligands involving three imidazole groups: $([Co(H_3L^6)](ClO_4)_3{\cdot}H_2O$ (**6**) and $[Co(H_3L^7)](ClO_4)_3{\cdot}0.5H_2O$ (**7**), H_3L^6 = tris[2-(((imidazol-4-yl)methylidene)amino)ethyl]amine and H_3L^7 = tris[2-(((2-methylimidazol-4-yl)methylidene)amino)ethyl]amine) (Figure 2a). Each complex induces the chirality of the *C* and *A* enantiomers due to the screw coordination arrangement of the achiral tripod-type ligand around the Co(III) ion (Figure 2b). The protonated complexes $[Co(H_3L^6)](ClO_4)_3{\cdot}H_2O$ (**6**) and $[Co(H_3L^7)](ClO_4)_3{\cdot}0.5H_2O$ (**7**), the formally hemi-deprotonated complexes $[Co(H_{1.5}L)](ClO_4)_{1.5}{\cdot}4H_2O$ (**6′**) and $[Co(H_{1.5}L^7)](ClO_4)_{1.5}$ (**7′**), and the fully deprotonated complexes $[Co(L^6)]{\cdot}2.5H_2O$ (**6″**) and $[Co(L^7)]{\cdot}3.5H_2O$ (**7″**) were obtained as good crystals by adjusting the pH of the solutions. The formally hemi-

(10) (a) Eliel, E. L. *Stereochemistry of Carbon Compounds*; McGraw-Hill: New York, 1962. (b) Collet, A.; Brienne, M.-J.; Jacques, J. *Chem. Rev.* **1980**, *80*, 215−230. (c) Jacques, J. J.; Collet, A.; Wilen, S. H. *Enantiomers, Racemates and Resolutions*; John Wiley & Sons: New York, 1981.
(11) Jacques, J.; Leclercq, M.; Brienne, M.-J. *Tetrahedron* **1981**, *37*, 1727−1733.
(12) Brock, C. P.; Schweizer, W. B.; Dunitz, J. D. *J. Am. Chem. Soc.* **1991**, *113*, 9811−9820.
(13) Kuroda, R.; Mason, S. F. *J. Chem. Soc., Dalton Trans.* **1981**, 1268−1273. (b) Brock, C. P.; Dunitz, J. D. *Chem. Mater.* **1994**, *6*, 1118−1127.
(14) (a) Hernandez-Molina, M.; Lloret, F.; Ruiz-Perez, C.; Julve, M. *Inorg. Chem.* **1998**, *37*, 4131−4135. (b) Lambert, F.; Renault, J.-P.; Policar, C.; M-Badaran, I.; Cesario, M. *Chem. Commun.* **2000**, 35−36.
(15) (a) Seto, C. T.; Whitesides, G. M. *J. Am. Chem. Soc.* **1993**, *115*, 905−916. (b) Bishop, R. *Synlett* **1999**, 1351−1358. (c) Aoyama, Y.; Endo, K.; Anzai, T.; Yamaguchi, Y.; Sawaki, T.; Kobayashi, K.; Kanehisa, N.; Hashimoto, H.; Kai, Y.; Masuda, H. *J. Am. Chem. Soc.* **1996**, *118*, 5562−5571.
(16) (a) Eliel, E. L.; Kofron, J. T. *J. Am. Chem. Soc.* **1953**, *75*, 4585−4587. (b) Addadi, L.; Lahav, M. *Pure Appl. Chem.* **1979**, *51*, 1269−1284.
(17) Miyasaka, H.; Okamura, S.; Nakashima, T.; Matsumoto, N. *Inorg. Chem.* **1997**, *36*, 4329−4335.
(18) (a) Mimura, M.; Matsuo, T.; Motoda, Y.; Matsumoto, N.; Nakashima, T.; Kojima, M. *Chem. Lett.* **1998**, 691−692. (b) Katsuki, I.; Matsumoto, N.; Kojima, M. *Inorg. Chem.* **2000**, *39*, 3350−3354.
(19) Kolks, G.; Frihart, C. R.; Rabinowitz, H. N.; Lippard, S. J. *J. Am. Chem. Soc.* **1976**, *98*, 5720−5721.
(20) Matsumoto, N.; Motoda, Y.; Matsuo, T.; Nakashima, T.; Re, N.; Dahan, F.; Tuchagues, J.-P. *Inorg. Chem.* **1999**, *38*, 1165−1173.
(21) Lorente, M. A. M.; Dahan, F.; Sanakis, Y.; Petrouleas, V.; Bousseksou, A.; Tuchagues, J.-P. *Inorg. Chem.* **1995**, *34*, 5346−5357.
(22) Shii, Y.; Motoda, Y.; Matsuo, T.; Kai, F.; Nakashima, T.; Tuchagues, J.-P.; Matsumoto, N. *Inorg. Chem.* **1999**, *38*, 3513−3522.
(23) Brewer, C. T.; Brewer, G.; Shang, M.; Scheidt, W. R.; Muller, I. *Inorg. Chim. Acta* **1998**, *278*, 197−201.

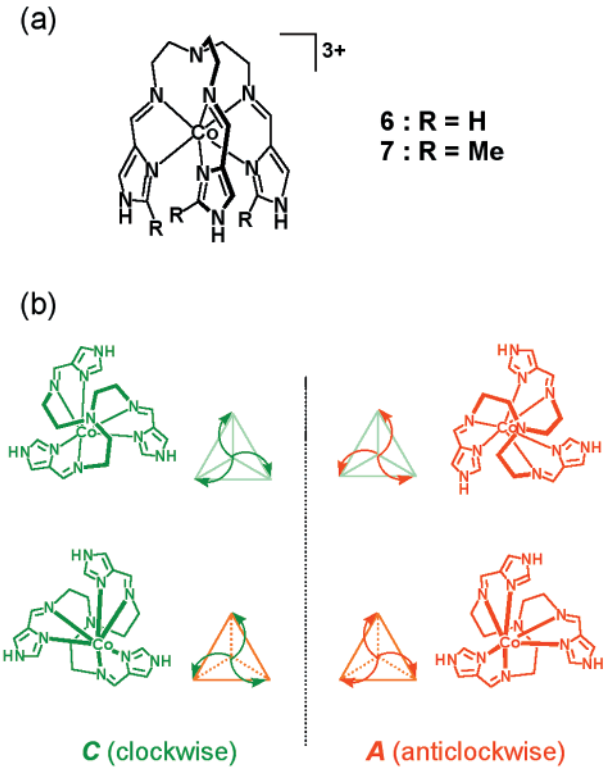

Figure 2. (a) Molecular structures of the cations of **6** and **7** $[Co(H_3L^n)]^{3+}$ (n = 6, 7). (b) Views looking down and up the molecule along the molecular C_3 axis for *C* (green) and *A* (red) enantiomers and their schematic representations, in which the curve line from the central tertiary amine to the terminal imidazole nitrogen through the imine nitrogen is represented by the arrow.

deprotonated species, $[Co(H_{1.5}L^n)]^{1.5+}$ (n = 6, 7), functions as a self-complementary chiral building block or generates equal numbers of completely protonated and completely deprotonated molecules $[Co(H_3L^n)]^{3+}$ and $[Co(L^n)]^0$ to form an extended 2D homochiral layer structure due to the intermolecular imidazole−imidazolate hydrogen bonds of the alternately arrayed $[Co(H_3L^n)]^{3+}$ and $[Co(L^n)]^0$. In this work, we report an interesting molecular system inducing spontaneous resolution, in which a chiral molecule generated from achiral components gives a homochiral 2D layer via self-organization and intermolecular homochiral interaction, and the resulting 2D layers with the same chirality are stacked in the crystal by fitting the up-and-down layer's shape to form a conglomerate.

Results and Discussion

Molecular Design of the Homochiral 2D Layer Structure. The Co(III) complex with tripod-type ligand involving three imidazole groups $[Co(H_3L^n)]^{3+}$ (n = 6, 7) was designed and synthesized. As shown in Figure 2, each complex has a molecular C_3 axis and induces the chirality of *C* and *A* enantiomers due to the screw coordination arrangement of the achiral tripod-type ligand. The Co(III) ion is inert for ligand substitution reactions, and hence the interconversion between *C* and *A* enantiomers through a trigonal twist mechanism (the so-called Bailar twist)[24] and through a bond rupture mechanism is restricted. From the adjustment of the pH of the solution containing the complex, the proper anionic salts of the protonated and the formally hemi-deprotonated complexes, $[Co(H_3L^n)]X_3$ and $[Co(H_{1.5}L^n)]X_{1.5}$ (n = 6, 7, X = mononegative ions), and the electrically neutral fully deprotonated complex, $[Co(L^n)]^0$, could be obtained. Among these, the hemi-deprotonated species $[Co(H_{1.5}L^n)]^{1.5+}$ functions as a chiral self-complementary building block or generates equal numbers of completely protonated and completely deprotonated molecules, $[Co(H_3L^n)]^{3+}$ and $[Co(H_3L^n)]^0$, by an acid−base reaction to form an extended 2D structure due to its intermolecular imidazole−imidazolate hydrogen bonds. Since the molecular building block having C_3 symmetry has a capped- and tripod-type molecular shape, and the adjacent molecules are linked by hydrogen bonds at the terminal sites of the molecules, the adjacent molecules are alternately arrayed on a plane perpendicular to the C_3 axes in an up-and-down fashion to give a 2D double-layer structure. As shown schematically in Figure 3, there are two pairs of plausible homochiral and heterochiral assembly 2D layer structures, in which one pair of structures (**a** and **b**) exhibits a trigonal void and the other pair of structures (**c** and **d**) exhibits a hexagonal void. As the frameworks of these 2D layer structures are constructed from multiple hydrogen bonds, there should be a distinct difference in the enantioselective discrimination between the homochiral and heterochiral aggregations. As experimentally confirmed later by the single-crystal X-ray analyses of the hemi-deprotonated complexes, **6′**, **6a′**, and **7′**, and as demonstrated later from molecular model considerations, the homochiral 2D assembly structure (**a**) is preferred to the other 2D structures (**b**, **c**, and **d**) in the present molecular system.

Synthesis and Properties of the Protonated, Hemi-deprotonated, and Fully Deprotonated Co(III) Complexes. The tripod-type hexadentate ligand H_3L^6 was prepared by mixing tris(2-aminoethyl)amine and 4-formylimidazole in a 1:3 molar ratio in methanol, and the ligand solution was used without isolation for the synthesis of the Co(III) complexes. The protonated Co(III) complex $[Co(H_3L^6)](ClO_4)_3 \cdot H_2O$ (**6**) was obtained as red-orange crystals by mixing the ligand solution, *trans*-$[CoCl_2(py)_4]Cl$,[25] and $NaClO_4$ in methanol in a 1:1:3 molar ratio, and from subsequent recrystallization of the crude product from aqueous solution at pH = 3. The C, H, and N microanalyses agreed with the formula $[Co(H_3L^6)](ClO_4)_3 \cdot H_2O$. The molar electrical conductivity in *N*,*N*-dimethylformamide (DMF) was 206 S mol^{-1} cm^2 and is in the expected range for a 1:3 electrolyte.[26] The IR spectrum showed the characteristic bands assignable to the C═N stretching vibration of the Schiff-base ligand at 1626 cm^{-1} and to the Cl−O vibration of the perchlorate ion at 1082−1145 cm^{-1}.[27] When 3 equiv of NaOH aqueous solution was added to a methanolic solution of **6**, the fully deprotonated complex **6″** with chemical formula $[Co(L^6)] \cdot 2.5H_2O$ was obtained as red cubic crystals. The IR spectrum showed a sharp band assignable to the C═N stretching vibration of the Schiff-base ligand at 1597 cm^{-1}, while the characteristic bands due to the perchlorate ion were absent. Compound **6″** was insoluble in common organic solvents and water, and hence measurement of the solution electrical conductivity could not be performed. When 1.5 equiv of aqueous NaOH solution, or triethylamine, was added to a methanolic solution of **6**, the hemi-deprotonated complex **6′** with the formal chemical formula $[Co(H_{1.5}L^6)](ClO_4)_{1.5} \cdot 4H_2O$, in which half of the three imidazole groups per unit are formally deprotonated, was obtained as

(24) Corey, E. J.; Bailar, J. C., Jr. *J. Am. Chem. Soc.* **1959**, *81*, 2620−2629.
(25) Werner, A.; Feenstra, R. *Ber. Dtsch. Chem. Ges.* **1906**, *39*, 1538−1545.
(26) Geary, E. J. *Coord. Chem. Rev.* **1971**, *7*, 81−122.
(27) Nakamoto, K. *Infrared and Raman Spectra of Inorganic and Coordination Compounds*, 4th ed.; John Wiley & Sons: New York, 1986.

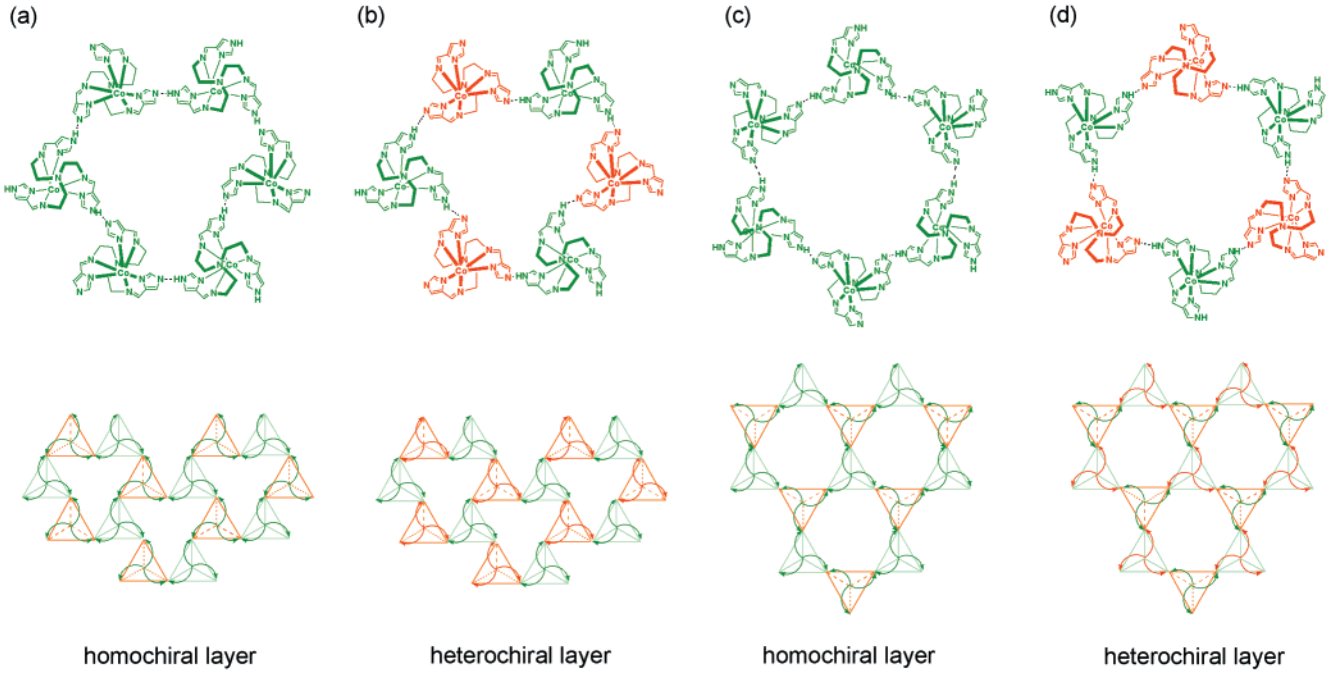

Figure 3. Two pairs of plausible homochiral and heterochiral assemblies formed by intermolecular imidazole−imidazolate hydrogen bonds between $[Co(H_3L^6)]^{3+}$ and $[Co(L^6)]^0$ with trigonal void (**a** and **b**) and with hexagonal void (**c** and **d**). (**a**) The molecular structure of a homochiral unit of the 2D layer of $\{[Co(H_3L^6)][Co(L^6)]\}_n$ and its schematic drawing with a trigonal void. (**b**) The molecular structure of a heterochiral unit and its schematic drawing with a trigonal void. (**c**) Homochiral unit structure with a hexagonal void and its schematic drawing. (**d**) Heterochiral unit structure with a hexagonal void and its schematic drawing. The color schemes are the same as for Figure 2.

orange crystals. The molar electrical conductivity in DMF was 129 S mol^{-1} cm^2, which is about half the value of **6** and consistent with the property of a formal 1:1.5 electrolyte.[26] In addition to the characteristic bands due to the perchlorate ion at 1059−1143 cm^{-1}, the IR spectrum showed two bands due to the C═N stretching vibration of the Schiff-base ligand at 1625 and 1594 cm^{-1}, which are assigned to the ν(C═N) of the protonated and deprotonated species, $[Co(H_3L^6)]^{3+}$ and $[Co(L^6)]^0$, respectively.

The Co(III) complex of the ligand H_3L^7 as the perchlorate salt, $[Co(H_3L^7)](ClO_4)_3\cdot 0.5H_2O$ (**7**), and the hemi-deprotonated and fully deprotonated complexes, $[Co(H_{1.5}L^7)](ClO_4)_{1.5}$ (**7′**) and $[Co(L^7)]\cdot 3.5H_2O$ (**7″**), were prepared by methods similar to those for the corresponding complexes **6**, **6′**, and **6″**, respectively. The molar electrical conductivities in ca. 10^{-3} M DMF solutions were 198, 111, and 0.7 S mol^{-1} cm^2 for **7**, **7′**, and **7″**, respectively, these values being consistent with their 1:3, 1:1.5, and neutral electrolyte properties, respectively.[26] The IR spectrum showed a characteristic band assignable to the C═N stretching vibration of the Schiff-base ligand at 1634 cm^{-1} for **7** and 1596 cm^{-1} for **7″**, respectively. The IR spectrum of **7′** showed two absorptions at 1635 and 1609 cm^{-1}, which are assignable to the ν(C═N) of the protonated and deprotonated species, $[Co(H_3L^7)]^{3+}$ and $[Co(L^7)]^0$, respectively.

Potentiometric pH Titration. To study the quantitative correlation between the pH and the proton dissociation−association of the imidazole groups, potentiometric pH titrations of **6** and **7** were performed in water. The proton association number, *n*, calculated using Bjerrum's method[28,29] vs pH is plotted for **6** and **7** in Figure 4a and b, respectively. The imidazole proton did not dissociate when **6** (or **7**) was dissolved in pure water (ca. 0.60×10^{-3} M aqueous solution), as indicated by the constant electrode potentials. The *n* value of **6** decreased from 3 to 0 for the forward titration with the addition of 0.05 M aqueous NaOH solution, in which the reddish transparent solution began to cloud, yielding a yellow precipitate around $n = 1.5$. For the reverse titration, the *n* value increased from 0 to 3 with the addition of 0.05 M HCl. The precipitate began to dissolve gradually, and the solution became transparent at $n = 1.5$. The reverse titration curve differs from the forward titration curve in the region of $n = 0-1.5$, probably due to the fact that **6″** is so insoluble and stable, such that protons could hardly bind to the imidazole group. The forward and reverse titration curves for **7** are almost the same, and precipitation was not observed under the experimental conditions. The pK_1, pK_2, and pK_3 values are 5.9, 7.2, and 8.5 for **6** and 6.3, 7.7, and 9.0 for **7**, respectively. The higher p*K* values in **7** are ascribed to the electron-donating effect of the 2-methyl group of the imidazole moiety. The fully protonated, the hemi-deprotonated, and the fully deprotonated complexes can be obtained as good quality crystals by adjusting the pH of the solution, based on the pH titration curves.

pH-Dependent Electronic Spectra. The pH-dependent electronic spectra of **7** were measured in aqueous solution (see Experimental Section), and the forward and reverse spectral change is shown in Figure 5a and b, respectively. The spectrum of **7** exhibited a broad band at 472 nm (molar extinction coefficient $\epsilon = 178$ M^{-1} cm^{-1}), assignable to a d−d transition. On addition of 0.10 M aqueous NaOH solution, the molar extinction coefficient of this broad band increased. This spectral change is characterized by isosbestic points at 418 and 554 nm. The spectra for the reverse titration exhibited isosbestic points at the same wavelengths and converted to the spectrum of the fully protonated complex **7**, demonstrating that the equilibrium is reversible. The pH-dependent electronic spectra of **6** were

(28) Gran, G. *Analyst* **1952**, *77*, 661−671.
(29) Beck, M. T.; Nagypal, I. *Chemistry of Complex Equilibria*; Wiley: New York, 1990; pp 243−286.

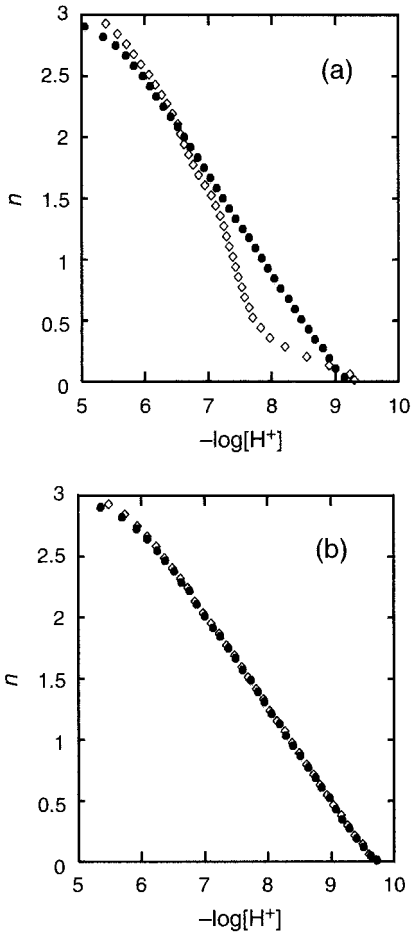

Figure 4. (a) The pH-dependent potentiometric titration curve in the plots of proton association number *n* vs pH of **6** for the forward (black) and reverse (white) titrations. (b) The pH-dependent potentiometric titration curve of **7**.

Table 1. Selected Coordination Bond Distances (Å) for $[Co(H_3L^6)](ClO_4)_3 \cdot H_2O$ (**6**), $[Co(H_{1.5}L^6)](ClO_4)_{1.5} \cdot 4H_2O$ (**6′**), $[Co(L^6)] \cdot 2.5H_2O$ (**6″**), and $[Co(H_{1.5}L^6)] \cdot 4H_2O$ (**6a′**)

	6	**6′**	**6″**	**6a′**
Co−N(2)	1.93(1)	1.90(2)	1.955(5)	1.961(9)
	1.94(1)	1.93(2)		1.980(9)
Co−N(3)	1.90(1)	1.92(2)	1.911(5)	1.905(8)
	1.94(1)	1.93(2)		1.896(8)
Co−N(5)	1.98(1)	1.88(2)		
	1.97(1)	1.99(2)		
Co−N(6)	1.88(1)	1.92(2)		
	1.92(1)	1.86(2)		
Co−N(8)	1.95(1)	1.98(2)		
	1.99(1)	2.03(2)		
Co−N(9)	1.91(1)	1.88(2)		
	1.908(8)	1.89(2)		

not measured, due to the precipitation encountered during the titration procedure.

X-ray Crystal Structures. The relevant coordination bond distances for (**6**, **6′**, **6″**, and **6a′**) and (**7**, **7′**, and **7″**) are summarized in Tables 1 and 2, respectively. The crystal data and details of the structure determination for **6**, **6′**, **6″**, and **6a′** and **7**, **7′**, and **7″** are summarized in Tables 3 and 4, respectively. Throughout the crystal structures of all of the complexes, each Co(III) ion assumes a similar octahedral coordination environment with the N_6 donor atoms of three Co−N(imidazole or imidazolate) bonds and three Co−N(imine) bonds. Each complex becomes a chiral molecule with a *C* or *A* enantiomer due

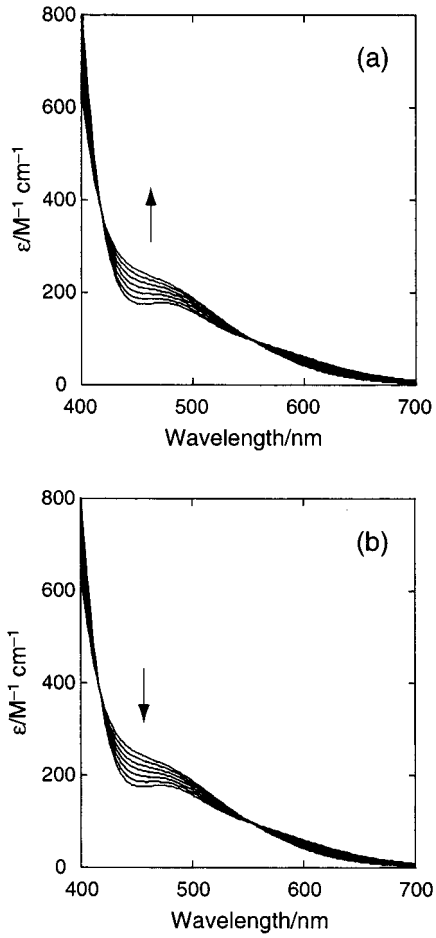

Figure 5. The pH-dependent electronic spectra of **7** for the (a) forward and (b) reverse titrations. An aqueous solution of **7** (0.24 mmol of the complex in 80 mL of water) was prepared. A spectrum was recorded after each 0.40 mL addition of 0.10 M NaOH solution, until 3 equiv of NaOH was added. Immediately afterward, the electronic spectra were recorded for the reverse titration, following each 0.40 mL addition of 0.10 M HCl solution to the solution resulting from the forward titration. The spectra were corrected for the volume variation due to the addition of the NaOH and HCl solutions.

Table 2. Relevant Coordination Bond Distances (Å) for $[Co(H_3L^7)](ClO_4)_3 \cdot 5H_2O$ (**7**), $[Co(H_{1.5}L^7)](ClO_4)_{1.5}$ (**7′**), and $[Co(L^7)] \cdot 3.5H_2O$ (**7″**)

	7	**7′**	**7″**
Co−N(2)	1.960(5), 1.967(5)	1.948(2),[a] 1.959(2)[b]	1.960(7)
Co−N(3)	1.944(5), 1.955(5)	1.942(2),[a] 1.945(2)[b]	1.919(7)
Co−N(5)	1.954(5), 1.945(5)		1.953(7)
Co−N(6)	1.934(5), 1.949(5)		1.933(7)
Co−N(8)	1.946(5), 1.947(5)		1.956(7)
Co−N(9)	1.952(5), 1.942(5)		1.940(7)

[a] Data for $[Co(H_3L^7)]^{3+}$. [b] Data for $[Co(L^7)]^0$.

to the screw coordination arrangement of the achiral tripod ligand around the Co(III) ion.

Structures of Protonated Co(III) Complexes 6 and 7. The crystal structures of **6** and **7** are essentially similar, and their structures can be adequately described as an isolated system. An ORTEP drawing of the cation of **6** is shown in Figure 6, representing the atom labeling and chiral coordination arrangement. There is no intermolecular hydrogen-bonded extended structure in the crystal structures of **6** and **7**. Their packing diagrams show that the *C* and *A* enantiomers coexist in the crystal to form a racemic compound. Figure 7 shows a packing

Table 3. X-ray Crystallographic Data for $[Co(H_3L^6)](ClO_4)_3\cdot H_2O$ (**6**), $[Co(H_{1.5}L^6)](ClO_4)_{1.5}\cdot 4H_2O$ (**6′**), $[Co(L^6)]\cdot 2.5H_2O$ (**6″**), and $[Co(H_{1.5}L^6)]Cl_{1.5}\cdot 4H_2O$ (**6a′**)

	6	**6′**	**6″**	**6a′**
formula	$C_{18}H_{26}N_{10}O_{13}Cl_3Co$	$C_{18}H_{30.5}N_{10}O_{10}Cl_{1.5}Co$	$C_{18}H_{26}N_{10}O_{2.5}Co$	$C_{18}H_{30.5}N_{10}O_4Cl_{1.5}Co$
fw	755.75	659.11	481.4	563.12
space group	*Cc* (No. 9)	*Cc* (No. 9)	$I\bar{4}3d$ (No. 220)	*P*3 (No. 143)
a, Å	36.389(2)	24.330(7)	20.446(1)	12.277(2)
b, Å	13.313(2)	12.887(5)	20.446(1)	12.277(2)
c, Å	12.704(2)	18.157(4)	20.446(1)	9.321(2)
α, deg	90	90	90	90
β, deg	104.98(1)	91.86(2)	90	90
γ, deg	90	90	90	120
V, Å^3	5946(1)	5690(3)	8546.6(2)	1216.7(2)
Z	8	8	16	2
D_{calc}, g cm^{-3}	1.688	1.539	1.496	1.537
μ, cm^{-1}	9.26	8.11	8.45	9.17
R,[a] R_w,[b] %	0.040, 0.045	0.060, 0.062	0.064, 0.037	0.055, 0.065

Table 4. X-ray Crystallographic Data for $[Co(H_3L^7)](ClO_4)_3\cdot 5H_2O$ (**7**), $[Co(H_{1.5}L^7)](ClO_4)_{1.5}$ (**7′**), and $[Co(L^7)]\cdot 3.5H_2O$ (**7″**)

	7	**7′**	**7″**
formula	$C_{21}H_{31}N_{10}O_{12.5}Cl_3Co$	$C_{21}H_{28.5}N_{10}O_6Cl_{1.5}Co$	$C_{21}H_{34}N_{10}O_{3.5}Co$
fw	788.83	629.13	541.50
space group	$P2_1/c$ (No. 14)	$R\bar{3}$ (No. 148)	*Fdd*2 (No. 43)
a, Å	13.195(4)	15.285(1)	23.112(3)
b, Å	13.873(5)	15.285(1)	35.397(2)
c, Å	33.930(4)	39.656(2)	12.425(2)
α, deg	90	90	90
β, deg	96.39(2)	90	90
γ, deg	90	120	90
V, Å^3	6172(3)	8024.1(5)	10164(2)
Z	8	12	16
$D_{calc.}$, g cm^{-3}	1.698	1.562	1.415
μ, cm^{-1}	8.95	8.49	7.22
R,[a] R_w,[b] %	0.058, 0.036	0.041, 0.032	0.048, 0.039

[a] $R = \sum||F_o| - |F_c||/\sum|F_o|$. [b] $R_w = [\sum w(|F_o| - |F_c|)^2/\sum w|F_o|^2]^{1/2}$, $w = 1/\sigma(F_o)^2$.

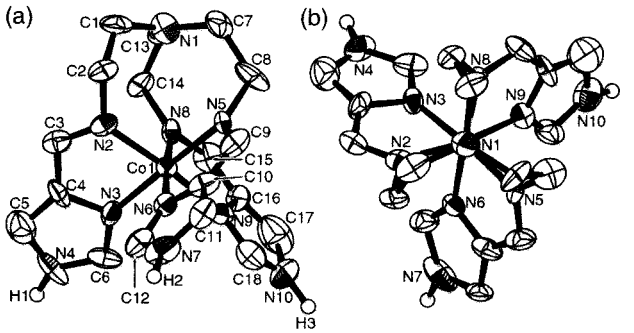

Figure 6. ORTEP drawings of the cation for $[Co(H_3L^6)](ClO_4)_3\cdot H_2O$ (**6**) with the selected atom numbering scheme showing 50% probability ellipsoids, in which one of the two crystallographically independent cations is represented. (a) The side view and (b) the top view projected from the central nitrogen atom to the Co^{3+} ion along the molecular C_3 axis showing the *C* enantiomer.

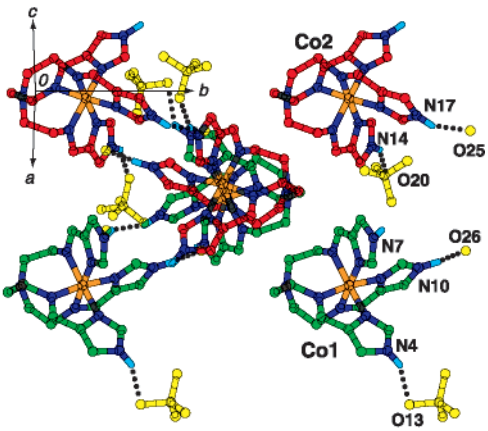

Figure 7. Packing diagram of $[Co(H_3L^6)](ClO_4)_3\cdot H_2O$ (**6**) showing that there is no extended intermolecular hydrogen-bonded network structure. Enantiomers *C* and *A* are represented by the colors green and red, respectively.

diagram of **6**, in which green- and red-colored molecules represent the *C* and *A* enantiomers, respectively.

The systematic extinction of the X-ray diffraction data of **6** indicated the space group to be either *C*2/*c* or *Cc*. When the space group *C*2/*c* was assumed, one of the three perchlorate ions of $[Co(H_3L^6)](ClO_4)_3\cdot H_2O$ suffered from disorder, and an occupancy factor of 0.5 must be assigned to both of the possible positions. Assuming the space group *Cc*, the structure has no disorder, and structural analysis gave better discrepancy indices than *C*2/*c*. The space group *Cc* was therefore selected. The crystal structure of $[Co(H_3L^6)](ClO_4)_3\cdot H_2O$ (**6**) consists of two electrically tripositive cations $[Co(H_3L^6)]^{3+}$, six ClO_4^- anions, and two water molecules of crystallization as the unique unit. Two of the three imidazole groups for each $[Co(H_3L^6)]^{3+}$ cation are hydrogen bonded to one oxygen atom of the ClO_4^- anions and one water molecule with hydrogen bond distances of N(4)···O(13) = 2.89(1) Å, N(10)···O(26) = 2.67(2) Å for cation Co(1) and N(14)···O(20) = 2.90(2) Å, N(17)···O(25) = 2.92(2) Å for cation Co(2). The water molecule O(25) is further hydrogen bonded to one oxygen atom of the ClO_4^- anion with O(25)···O(21) = 2.69(2) Å.

The complex $[Co(H_3L^7)](ClO_4)_3\cdot 0.5H_2O$ (**7**) crystallized into the monoclinic space group $P2_1/c$ with $Z = 8$. The crystal structure consists of two electrically tripositive $[Co(H_3L^7)]^{3+}$ cations, six ClO_4^- anions, and one water molecule of crystallization as the unique unit. One of the three imidazole nitrogen atoms of the first cation Co(1) is hydrogen bonded to one perchlorate anion with N(7)···O(1) = 2.892(8) Å. Three imid-

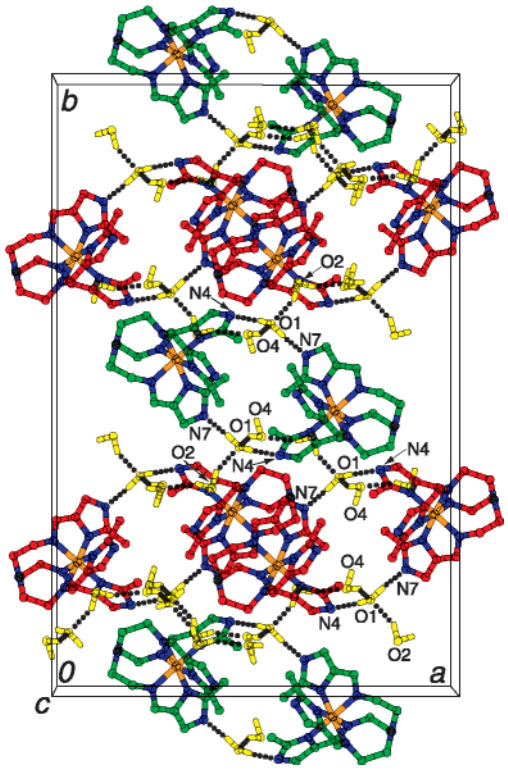

Figure 8. An extended intermolecular hydrogen-bonded network structure of $[Co(L^7)]\cdot 3.5H_2O$ (**7″**). The water oxygen atom O(1) and the atom O(1)* generated by a two-fold rotation symmetry operation doubly bridge the two adjacent $[Co(L^7)]$ and $[Co(L^7)]$* species by hydrogen bonds to give a hydrogen-bonded dimeric structure. Enantiomers *C* and *A* are represented by the colors green and red, respectively.

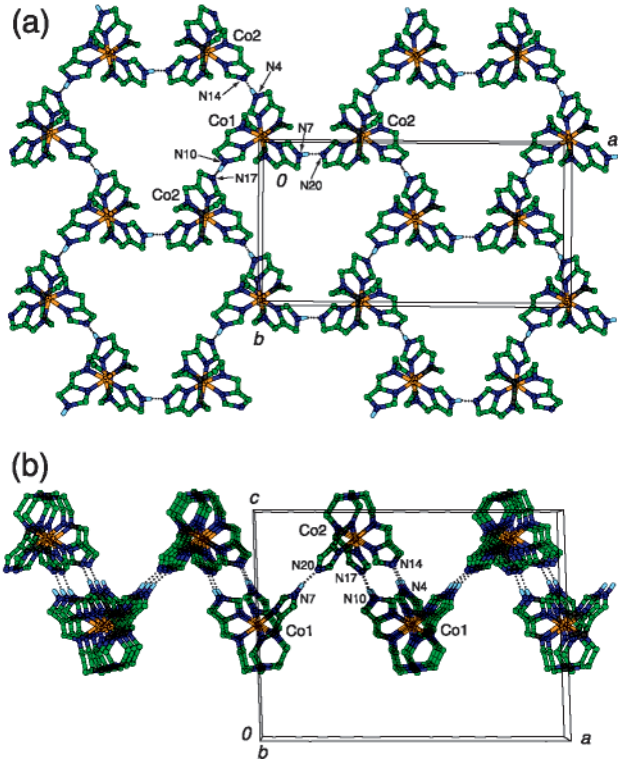

Figure 9. X-ray crystal structure of $[Co(H_{1.5}L^6)](ClO_4)_{1.5}\cdot 4H_2O$ (**6′**) showing a homochiral 2D layer structure formed by hydrogen bonds between $[Co(H_3L^6)]^{3+}$ (Co1) and $[Co(L^6)]^0$ (Co2) (dashed line). The counteranions and the water molecules are omitted for clarity. (a) Top view showing a layer structure, in which the same enantiomers (*C*, green) are linked by intermolecular imidazole−imidazolate hydrogen bonds. (b) Side view of a double layer consisting of an up-and-down molecular array.

azole nitrogen atoms of the second cation Co(2) are hydrogen bonded to the water molecule and two independent perchlorate ions with N(14)···O(26) = 2.762(7) Å, N(17)···O(9) = 2.835 (7) Å, and N(20)···O(13) = 2.857(7) Å, respectively. The water molecule O(26) is further hydrogen bonded to the oxygen atom of another perchlorate ion with O(26)···O(18) = 2.825(7) Å.

Structures of Fully Deprotonated Co(III) Complexes 6″ and 7″. Both **6″** and **7″** form a hydrogen-bonded network structure through water molecules. The fully deprotonated complex $[Co(L^6)]\cdot 2.5H_2O$ (**6″**) crystallized in the cubic space group $I\bar{4}3d$ with $Z = 16$, and thus, one-third of the molecule is the unique unit. The Co(III) ion and the central amine nitrogen atom occupy special positions passing through the C_3 axis. The water molecule suffers from disorder, and the occupancy factor was assigned to the oxygen atom. The imidazolate nitrogen atoms of $[Co(L^6)]^0$ are hydrogen bonded to the crystal water molecule with a bond distance of N(4)···O(1) = 2.766(9) Å. The neighboring water molecules are further hydrogen bonded to each other to form an extended intermolecular network structure.

The fully deprotonated complex $[Co(L^7)]\cdot 3.5H_2O$ (**7″**) crystallized in the orthorhombic space group *Fdd*2, consisting of $[Co(L^7)]\cdot 3.5H_2O$ as the unique unit, and the crystal structure is shown in Figure 8. The water oxygen atom O(1) and the atom O(1)* generated by a two-fold rotation symmetry operation doubly bridge the two adjacent $[Co(L^7)]$ and $[Co(L^7)]$* species by hydrogen bonds with N(4)*···O(1) = 2.92(1) Å and N(7)···O(1) = 2.830(9) Å to give a hydrogen-bonded dimeric structure. The oxygen atom O(1) is further hydrogen bonded to other water molecules with the distances of O(1)···O(2) = 2.90(1) Å and O(1)···O(4) = 2.89(1) Å, and the two oxygen atoms O(2) and O(4) are hydrogen bonded with O(2)···O(4) = 2.90(1) Å. As a result, an extended dimensional structure is constructed due to these hydrogen bonds.

Structures of Hemi-deprotonated Co(III) Complexes 6′ and 7′. The crystal structures of **6′** and **7′** consist of an essentially similar 2D layer, constructed from the intermolecular imidazole−imidazolate hydrogen bonds. Figure 9 shows the top view and the side view of the 2D layer structure of **6′**, in which the perchlorate anions and the water molecules are omitted for clarity.

The systematic extinction of the X-ray diffraction data of **6′** suggested either the space group *C*2/*c* or *Cc*. Both structural analyses gave acceptable solutions for the space groups *C*2/*c* and *Cc* under the condition that some disorder was included. The X-ray analyses could not determine the space group definitely due to the small number of observed reflections, where oxygen atoms of perchlorate ions and water molecules were refined with the isotropic thermal parameter and all of the hydrogen atoms were placed at their calculated positions. The space group *Cc* was finally selected on the basis of chemical and physical reasons. The unique unit in the space group *Cc* involves a fully deprotonated complex and a fully protonated complex as well as three ClO_4^- ions, whereas the unique unit in the space group *C*2/*c* consists of $[Co(H_{1.5}L^6)]^{1.5+}$ and 1.5 ClO_4^- anion. The infrared spectrum showed two bands assignable to the protonated and deprotonated species, which supports the space group *Cc*. Further, the X-ray structure of the analogous compound **7′** described later was definitely solved by the formulation $[Co(H_3L^7)][Co(L^7)](ClO_4)_3$.

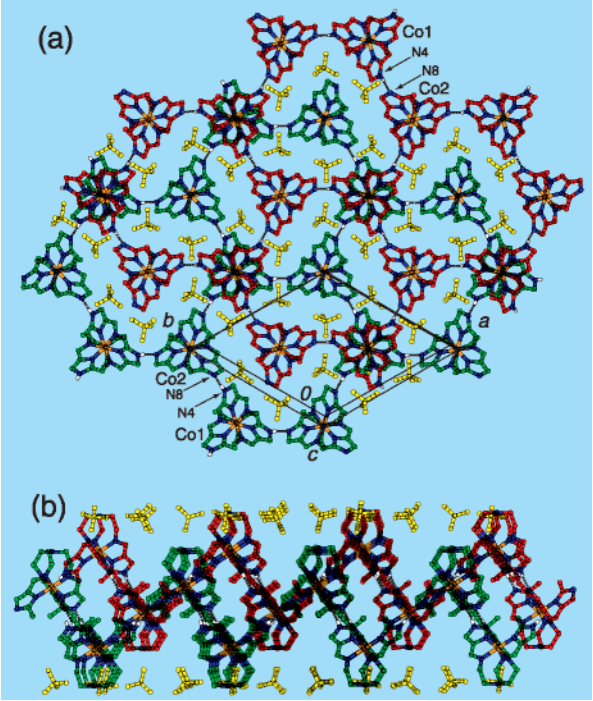

Figure 10. X-ray crystal structure of $[Co(H_{1.5}L^7)](ClO_4)_{1.5}$ (**7′**) showing a homochiral 2D layer structure. Two complementary molecular building blocks with the same chirality, i.e., the protonated species $[Co(H_3L^7)]^{3+}$ (*A* enantiomer, red) and the fully deprotonated species $[Co(L^7)]^0$ (*A* enantiomer, red), are linked by the intermolecular hydrogen bond of N(4)···N(8) = 2.725(4) Å and arrayed alternately in an up-and-down fashion to give a homochiral 2D layer structure. (a) Top view showing the stacking manner of two adjacent layers with opposite chirality and showing no channel structure. (b) Side view.

The crystal structure of **6′** consists of a completely protonated complex $[Co(H_3L^6)]^{3+}$, a completely deprotonated complex $[Co(L^6)]^0$, three perchlorate anions, and eight water molecules of crystallization as the unique unit. The component molecules $[Co(H_3L^6)]^{3+}$ and $[Co(L^6)]^0$ are chiral molecules with the *C* or *A* screw coordination arrangement of the tripod ligand. They function as chiral complementary building blocks and aggregate alternately due to the intermolecular imidazole−imidazolate hydrogen bonds to form an extended 2D layer structure having a hexanuclear unit with a trigonal void, as shown in Figure 9a. The intermolecular N···N hydrogen bond distances are N(4)···N(14) = 2.72(3), N(7)···N(20) = 2.703(13), and N(10)···N(17) = 2.68(3) Å. The adjacent molecules with a capped- and tripod-type shape are arrayed in an alternate up-and-down fashion to give a double-layer structure, as shown in Figure 9b.

Figure 10 shows the top and side views of the crystal structure of the homochiral 2D layer for the methyl substituent at the 2-position of the imidazole moiety, $[Co(H_{1.5}L^7)](ClO_4)_{1.5}$ (**7′**). **7′** crystallized in the trigonal centrosymmetric space group $R\bar{3}$, and the crystal structure consists of a completely protonated species $[Co(H_3L^7)]^{3+}$, a completely deprotonated species $[Co(L^7)]^0$, three perchlorate anions, in which the unique atoms are one-third of $[Co(H_3L^7)]^{3+}$ and $[Co(L^7)]^0$, and one perchlorate ion. Since the hydrogen atoms were refined well by the least-squares calculation, the protonated and deprotonated molecules are well distinguished by the X-ray analysis. Two component molecules, $[Co(H_3L^7)]^{3+}$ and $[Co(L^7)]^0$, having molecular C_3 axes are arrayed alternately in an up-and-down fashion on a plane perpendicular to the C_3 axis and are linked by the intermolecular imidazole−imidazolate hydrogen bond of N(4)···N(8) = 2.725(4) Å to give a 2D layer structure, in which the component molecules $[Co(H_3L^7)]^{3+}$ and $[Co(L^7)]^0$ with the same chirality are assembled. The Co−N(imine) and Co−N(imidazole) coordination bond distances for the protonated species Co(1) are 1.948(2) and 1.942(2) Å, respectively, and those for the deprotonated species Co(2) are 1.959(2) and 1.945(2) Å, respectively, demonstrating that the Co−N(imine) distance is greatly affected by the deprotonation and the Co−N(imine) distance for the deprotonated molecule is rather longer than that for the protonated molecule. In contrast to the Co−N(imine) distance, the C═N bond distance 1.273(3) Å for the protonated molecule is slightly shorter than that for the deprotonated molecule, 1.288(4) Å. This result is consistent with the infrared spectrum, which exhibits two bands at 1635 and 1609 cm^{-1} assignable to the C═N vibrations of the protonated and deprotonated molecules, respectively, as described previously. Figure 10 shows that a homochiral layer with *C* enantiomer and an adjacent layer with *A* enantiomer are stacked alternately, and there is no channel structure.

The most striking feature of the crystal structures **6′**, **7′**, and **6a′** (described later) is that the *C* enantiomer aggregates only with the *C* enantiomer and the *A* enantiomer aggregates only with the *A* enantiomer to produce a homochiral assembled 2D layer.

Consideration of Plausible Homochiral and Heterochiral 2D Layer Structures. Figure 3 shows two pairs of plausible homochiral and heterochiral 2D layer structures, in which one pair (**a** and **b**) exhibits a trigonal void and the other pair (**c** and **d**) exhibits a hexagonal void. The X-ray analyses of **6′** and **7′** reveal that the compounds assume the homochiral 2D layer structure with a trigonal void (**a**) and that the structure is suitable for hydrogen bond formation. The heterochiral 2D layer structure with a trigonal void (**b**) is unfavorable on the basis of molecular model considerations. When one of two adjacent molecules of the 2D layer structure (**a**) in Figure 9 was replaced by an alternating chiral molecule in order to have the same NH···N distance, structure (**b**) resulted. The directions of the two adjacent imidazole and imidazolate moieties are apparently unsuitable for the formation of a hydrogen bond.

There is the other pair of plausible 2D layer structures with a hexagonal void (**c** and **d**), in which each triangle representing the tripod C_3 geometry of the complex is arrayed on a plane perpendicular to the C_3 axis in an alternate up-and-down fashion to form a layered structure consisting of a hexanuclear structure with a hexagonal void as a unit. On the other hand, each triangle of (**a** and **b**) is arrayed in the same direction on a plane perpendicular to the C_3 axis to form a layer structure consisting of a hexanuclear structure with a triangle void. Therefore, a pair of the structures (**a** and **b**) is geometrically different from the other pair of the structures (**c** and **d**). On the basis of similar molecular model considerations, we can easily anticipate that the heterochiral 2D layer structure (**d**) is much preferred to the homochiral layer structure (**c**). The above consideration suggests that the homochiral aggregation would lead to a structure with a trigonal void (**a**) and that the heterochiral aggregation would lead to a structure with a hexagonal void (**d**). At present, we do not have enough data to conclude that the homochiral structure (**a**) is preferred to the heterochiral structure (**d**).

The relationship between the molecular chirality and the assembly structure has been well investigated for the oxalato-

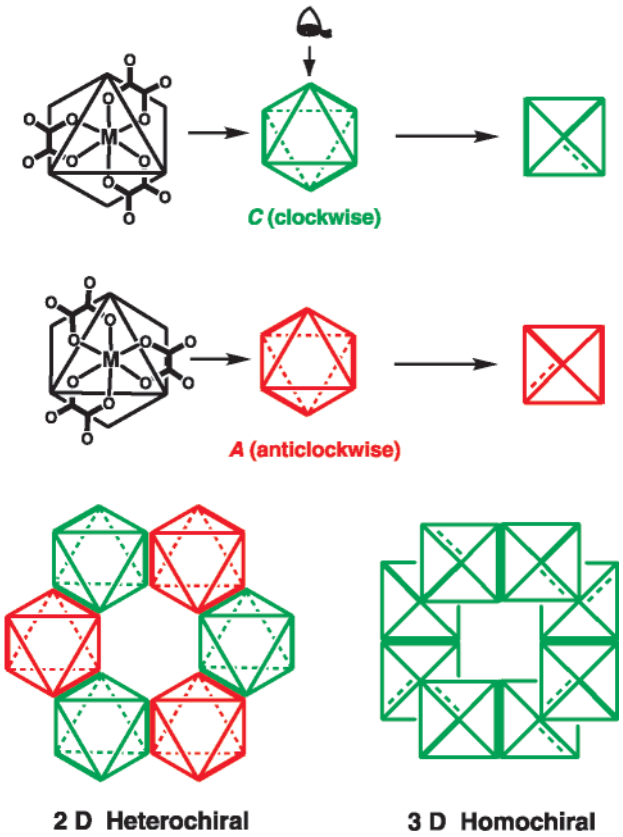

Figure 11. Relationship between the molecular chirality of the building blocks and the assembly structure for the oxalato-bridged heterometal assembly $[MM'(ox)_3]_n$. The building components $[M(ox)_3]$ and $[M'(ox)_3]$, represented by chiral octahedra, assume a $\Delta(C)$ or $\Lambda(A)$ configuration. The geometrically different 3D and 2D structures are constructed by the homochiral and heterochiral assemblies of the chiral building components $[M(ox)_3]$ and $[M'(ox)_3]$, respectively.

bridged heterometal assembly compounds $[MM'(ox)_3]_n$, in which the building components $[M(ox)_3]$ and $[M'(ox)_3]$, represented by chiral octahedra, have D_3 symmetry and assume a $\Delta(C)$ or $\Lambda(A)$ configuration.[30−32] Figure 11 shows schematic drawings of the chiral building components and the generated assembly structures. When the building components with the same chirality $[M(ox)_3]$ and $[M'(ox)_3]$ are alternately arrayed by an oxalato bridge, a homochiral 3D assembly structure is generated.[31] When the components with different chirality are alternately arrayed, a heterochiral 2D honeycomb layer structure is generated.[31] This demonstrates that the homochiral and heterochiral assembling of chiral building components $[M(ox)_3]$ and $[M'(ox)_3]$ produced geometrically different 3D and 2D structures, respectively. As examined above, the molecular model consideration of our complementary components $[Co(H_3L^n)]^{3+}$ and $[Co(L^n)]^0$ suggests that the homochiral aggregation would lead to a structure with a trigonal void (**a**), while the heterochiral aggregation would lead to a structure with a hexagonal void (**d**). This demonstrates that the homochiral aggregation also produces a structure that is geometrically different from that of the heterochiral aggregation in the present molecular system.

Formation of the Conglomerate by Tuning Counteranions. The homochiral 2D layer structure is preferentially constructed by multiple intermolecular hydrogen bonds in this molecular system. There are two possible stacking manners of the 2D layers into the 3D crystal lattice. In both of the crystal lattices of **6′** and **7′**, a homochiral layer with *C* enantiomer and an adjacent homochiral layer with *A* enantiomer are stacked alternately to give a heterochiral interlayer crystal packing. The counteranion occupies a part of the interlayer space, so it is expected that the stacking manner of the 2D layers into the 3D crystal lattice depends somewhat on the size and shape of the counteranion. It is known that the chloride and bromide salts of chiral cobalt(III) complexes, $[Co(ox)en_2]X$ and *cis*-$[Co(NO_2)_2en_2]X$ (X = Cl^-, Br^-, I^-, ox = oxalato, en = ethylenediamine), exhibit spontaneous resolution but the iodide salts do not exhibit spontaneous resolution.[33] This suggests that a homochiral crystal stacking can be obtained by choosing the proper counteranions.

In this molecular system, the small counteranionic salts, such as the chloride and nitrate salts, gave the homochiral interlayer stacking of 2D homochiral layers into the 3D crystal lattice. The chloride salt $[Co(H_{1.5}L^6)]Cl_{1.5}\cdot 4H_2O$ (**6a′**) crystallized in a noncentrosymmetric trigonal space group *P*3 with $Z = 2$. The complex forms a homochiral 2D layer structure constructed by multiple intermolecular hydrogen bonds between the completely protonated and completely deprotonated components $[Co(H_3L^6)]^{3+}$ and $[Co(L^6)]^0$, similar to those of **6′** and **7′**, in which the imidazole−imidazolate hydrogen bond distance is N(4)···N(8) = 2.701(11) Å and the hydrogen atoms were placed at their calculated positions. Figure 12a shows the stacking manner of the homochiral 2D layers of **6a′** projected along the C_3 axis (crystallographic *c*-axis), in which the adjacent layers with the same chirality are stacked along the *c*-axis without shift by fitting and adopting the up-and-down shaped layers themselves to give a channel structure and to form a chiral crystal. Figure 12b shows the side view of the homochiral 2D layers of **6a′**, in which the Cl^- ions are accommodated in the intermediate region of the double layer. The water molecules exist as the crystal water and play no role in hydrogen bonding. The distance of Co(1)···Co(2) bridged by the intermolecular NH···N hydrogen bond is 10.405(2) Å, and the next neighboring Co···Co distances of an intralayer hexagonal unit are Co(1)···Co(1) = Co(2)···Co(2) = 12.277(2) Å. One Co(III) ion of one layer is contacted by five Co(III) ions of adjacent layers. These five interlayer Co···Co contact distances without the NH···N bridge are composed of three contact distances at 7.290(2) Å due to contact parallel to the layer and two contacts at 9.321(2) Å due to contact perpendicular to the layer. The intra- and interlayer Co···Co distances for **6′**, **6a′**, and **7′** are summarized in Table 5.

In a comparison of homochiral stacking with heterochiral stacking of the 2D layer into the 3D lattice, Figure 13a shows the top view of the stacking manner of **6′** projected along the C_3 axis, in which the adjacent layers with opposite chirality are stacked. Figure 13b shows the side view of the heterochiral stacking of 2D layers of **6′**, demonstrating that the ClO_4^- ions are positioned in a cavity. As given in Table 5, the intralayer Co(1)···Co(2) distances bridged by the hydrogen bonds are 10.412(5), 10.367(3), and 10.365(5) Å for **6′**, and 10.849(1) Å

(30) Tamaki, H.; Zhong, Z. J.; Matsumoto, N.; Kida, S.; Koikawa, M.; Achiwa, N.; Hashimoto, Y.; Okawa, H. *J. Am. Chem. Soc.* **1992**, *114*, 6974−6979.
(31) Decurtins, S.; Schmalle, H. W.; Oswald, H. R.; Linden, A.; Ensling, J.; Gütlich, P.; Hauser A. *Inorg. Chim. Acta* **1994**, *216*, 65−73.
(32) Decurtins, S.; Schmalle, H. W.; Schneuwly, P.; Oswald, H. R. *Inorg. Chem.* **1993**, *32*, 1888−1892.
(33) (a) Cai, J.; Myrczek, J.; Bernal, I. *J. Chem. Soc., Dalton Trans.* **1995**, 611−619. (b) Yamanari, K.; Hidaka, J.; Shimura, Y. *Bull. Chem. Soc. Jpn.* **1973**, *46*, 3724−3728. (c) Gillard, R. D.; Tipping, L. H. R. *J. Chem. Soc., Dalton Trans.* **1977**, 1241−1247.

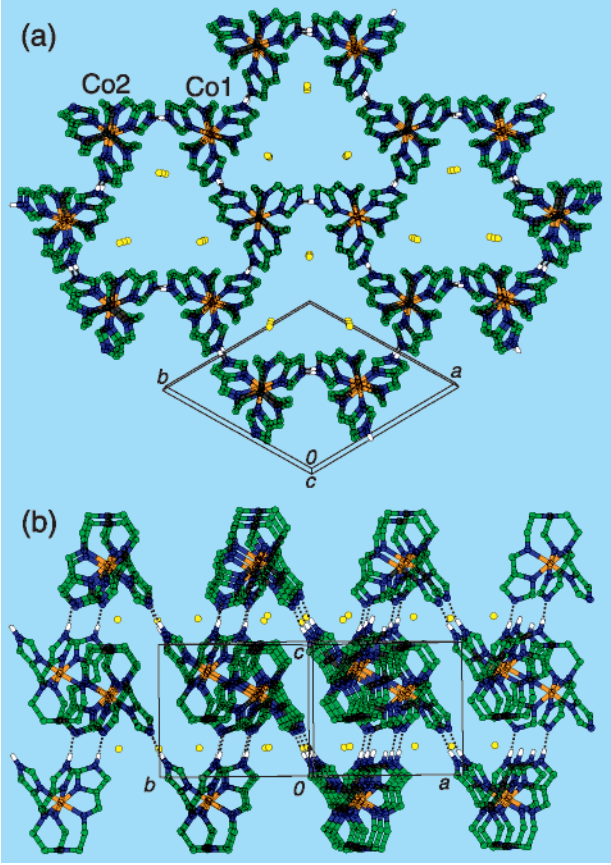

Figure 12. Stacking manner of two adjacent layers of the homochiral 2D layer complex $[Co(H_{1.5}L^6)]Cl_{1.5}\cdot 4H_2O$ (**6a′**) with an intermolecular imidazole−imidazolate hydrogen bond distance of N(4)···N(8) = 2.701(11) Å. Adjacent layers with the same chirality (*C* enantiomers, green) are stacked along the *c*-axis by fitting or adopting the up-and-down layer's shape to form a channel. The Cl^- ions (yellow), as the counteranion, are located in the intermediate region of the double layer. (a) Top view showing the channel structure. (b) Side view showing the positions of the Cl^- ions.

Table 5. Intra- and Interlayer Co···Co Distances (Å) for 2D Assembly Compounds $[Co(H_{1.5}L^6)](ClO_4)_{1.5}\cdot 4H_2O$ (**6′**), $[Co(H_{1.5}L^6)]\cdot 4H_2O$ (**6a′**), and $[Co(H_{1.5}L^7)](ClO_4)_{1.5}$ (**7′**)

	6′	6a′	7′
(a) Intralayer Co···Co Distances of Hexagon Unit (Å)			
Co(1)···Co(2) (bridged by NH···N)	10.367(3) 10.365(5) 10.412(5)	10.405(2)	10.849(1)
Co···Co (next neighbor)	12.887(3) 13.766(3)	12.277(2)	15.285(1)
(b) Interlayer Co···Co Distances (Å)			
Co(1)···Co(1)	9.099(2)	9.321(2)	9.4236(7) 9.914(1)
Co(2)···Co(2)	9.105(2)	9.321(2)	9.2303(6) 10.514(1)
Co(1)···Co(2)	8.490(3) 8.388(3) 7.431(3)	7.290(2)	9.614(1) 9.5328(6)

for **7′**, which are compatible with 10.405(2) Å of **6a′**. The three next neighboring intralayer Co···Co distances of the hexagonal structure are 12.887(3) Å and two 13.766(3) Å for **6′**, and 15.285(1) Å for **7′**, which are significantly longer than 12.277(2) Å of **6a′**. These data demonstrate that the dimensions of the hexagon of one layer can be easily deformed and expanded by the counteranion and the methyl group at the imidazole moiety, suggesting that the 2D hydrogen-bonding network is surprisingly and conveniently flexible.

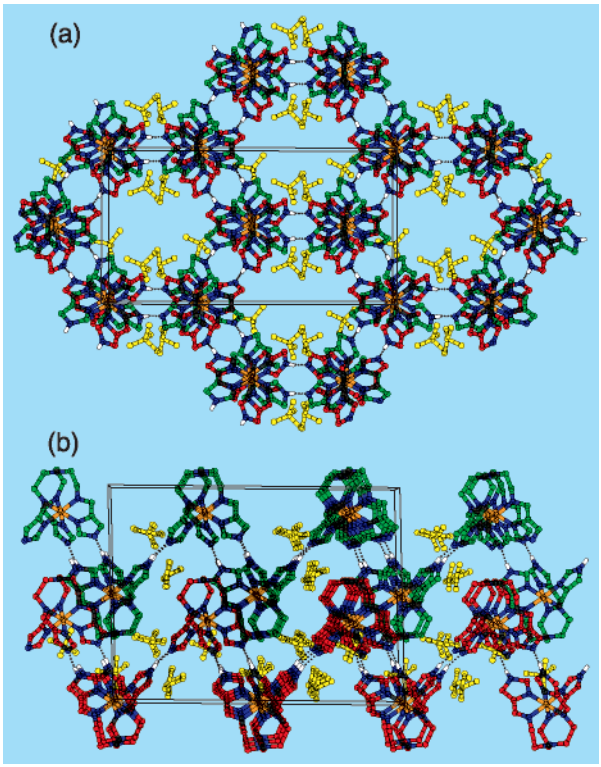

Figure 13. Stacking manner of two adjacent layers of the heterochiral 2D layer complex $[Co(H_{1.5}L^6)](ClO_4)_{1.5}\cdot 4H_2O$ (**6′**), in which adjacent layers with different chirality (*C* enantiomer, green, and *A* enantiomer, red) are alternately stacked, and the ClO_4^- ions (yellow) are located approximately in the cavity. (a) Top view. (b) Side view showing the positions of the ClO_4^- ions.

The interlayer Co···Co contact distances perpendicular to the layers are 9.009(2) and 9.105(2) Å for **6′** and 9.4236(7) and 9.2303(6) Å for **7′**, which are compatible with 9.321(2) Å of **6a′**. The three interlayer Co···Co distances parallel to one layer are 7.431(3), 8.388(3), and 8.490(3) Å for **6′** and 9.614(1), 9.914(1), and 9.5328(6) Å for **7′**. These distances are significantly longer than 7.290(2) Å of **6a′**, indicating that a closer interlayer packing is achieved in **6a′**. A rather bulky counteranion, such as ClO_4^-, cannot be accommodated in the intermediate region of the double layer but occupies the interlayer space. The data demonstrate that the hexagonal unit of the 2D layer of **6′** spreads out and elongates to one direction, to avoid the perchlorate ions. The hexagonal unit of the 2D layer of **7′** also spreads out due to the steric requirement of the 2-methyl group of the imidazole moiety, and a 2D layer is stacked on the adjacent layer with opposite chirality and shift, as shown in Figure 10. As shown in Figure 12, the Cl^- ions of **6a′** are located in the intermediate region of the double layer, and therefore the adjacent layers of **6a′** are stacked closer than in **6′** by fitting and adopting the up-and-down shape's layers, as evidenced by the interlayer distances. In other words, a close interlayer stacking can be achieved for the 2D compound with the smaller counteranion and leads to a homochiral interlayer stacking into a 3D lattice to induce a conglomerate.

Circular Dichroism Spectra. The X-ray analysis demonstrates that **6a′** is a conglomerate and that spontaneous resolution of the two enantiomers occurs during the course of the crystallization. A crystal of **6a′** was selected and dissolved in dimethyl sulfoxide. The circular dichroism (CD) spectrum of the solution was measured in the range 330−600 nm. The

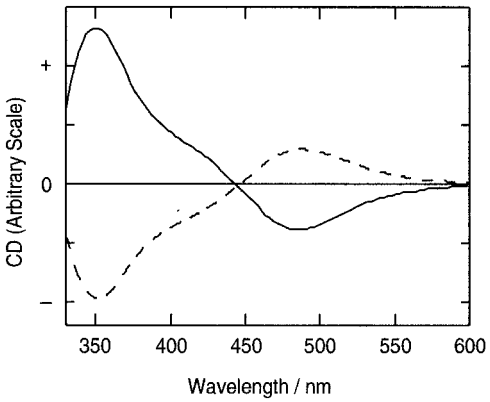

Figure 14. CD spectra of a crystallite of **6a′** dissolved in dimethyl sulfoxide. The CD spectrum (solid curve) was measured in the range 330−600 nm. Another crystal showed an enantiomeric CD pattern (dotted curve).

spectrum showed a positive peak and a negative peak at 480 and 350 nm, respectively, and the spectrum of another crystal showed an enantiomeric CD pattern. The CD spectra of the two crystals of **6a′** are shown in Figure 14. The observation of the Cotton effect provides definitive evidence that spontaneous resolution took place during the course of crystallization.

Concluding Remarks. This work shows an example of evolution in chirality, that is, the progression from the synthetically simple achiral ligand, to the isolated chiral complex, to the homochiral assembled 2D layer, and then to the conglomerate. The synthesized Co(III) complexes with capped- and tripod-type ligands containing three imidazole groups, $[Co(H_3L^n)]^{3+}$ ($n = 6, 7$), contain the relevant molecular information required to answer the molecular design question, "how to generate chirality from achiral components and how to force racemates of chiral molecules to undergo spontaneous resolution", from (1) a generation of molecular chirality due to the screw coordination arrangement of an achiral ligand around a metal ion, (2) a self-organization process derived from their self-complementary character, and (3) an extended multidimensional homochiral discrimination in a self-organization process. The complexes have a molecular C_3 axis and induce the chirality of *C* and *A* enantiomers due to the screw coordination arrangement of the achiral tripod ligand around the Co(III) ion. By adjustment of the pH of the solution, the species with the formal chemical formula of $[Co(H_{1.5}L^n)]^{1.5+}$ generates equal numbers of completely protonated and completely deprotonated molecules as chiral complementary building blocks to form a 2D homochiral layer structure formed by intermolecular imidazole−imidazolate hydrogen bonds on crystallization. The chiral molecular blocks are linked by multiple hydrogen bonds and are arrayed on a plane perpendicular to the molecular C_3 axes in an alternate up-and-down fashion to produce a unique 2D double-layer structure. The counteranion, together with the crystal solvent molecules, occupies a part of the interlayer space so that the packing manner of the homochiral 2D layers depends somewhat on the size of the counteranion. Smaller counteranions, such as Cl^-, can be accommodated in the intermediate region of the double layer and thus lead to a tight homochiral interlayer stacking. In the presence of a small counteranion, the hemi-deprotonated complex undergoes spontaneous resolution. The present molecular design can provide a novel synthetic design of homochiral porous materials for enantioselective separation and catalysis.[4] Although the size of the chiral void is small in the present complexes, the chiral void space can be tuned by introducing a proper spacer molecule. Another noteworthy property of this molecular system is that the interconversion between the building blocks and the 2D homochiral assembly framework with a chiral void is reversible by adjustment of the pH. A study along this line is currently underway.

Experimental Section

Caution! Perchlorate salts of metal complexes with organic ligands are potentially explosive. Only small quantities of material should be prepared, and the samples should be handled with care.

General Procedure. All chemicals and solvents used in the syntheses were of reagent grade. Reagents used for the physical measurements were of spectroscopic grade.

Tris[2-(((imidazoyl-4-yl)methylidene)amino)ethyl]amine H_3L^6. Tris(2-aminoethyl)amine (0.146 g, 1 mmol) was added to a solution of 4-formylimidazole (0.288 g, 3 mmol) in 30 mL of methanol, and the mixture was stirred at 50 °C for 10 min. The ligand solution was used without any isolation of the ligand for the synthesis of the cobalt(III) complexes.

$[Co(H_3L^6)](ClO_4)_3\cdot H_2O$ (6). Tris(2-aminoethyl)amine (0.146 g, 1 mmol) was added to a solution of 4-formylimidazole (0.288 g, 3 mmol) in 30 mL of methanol, and the mixture was stirred at 50 °C for 10 min. A solution of *trans*-$[CoCl_2(py)_4]Cl$[24] (0.482 g, 1 mmol) in 20 mL of methanol was added to the ligand solution. After the first solution was stirred for 1 h at room temperature, a solution of $NaClO_4$ (0.367 g, 3 mmol) in 15 mL of methanol was added. The mixed solution was filtered, and the filtrate was allowed to stand overnight. The dark red crystalline precipitate was collected by suction filtration, washed with a small volume of methanol, and dried in vacuo. Recrystallization was performed from the aqueous solution at pH = 3, adjusted by the addition of 0.10 M HCl. Yield: 0.242 g (42%). Anal. Calcd for $[Co(H_3L^6)](ClO_4)_3\cdot H_2O$: C, 28.61; H, 3.47; N, 18.53. Found: C, 28.64; H, 3.48; N, 18.69. IR (KBr): $\nu_{C=N}$(imine), 1626 cm^{-1}; $\nu_{Cl-O}(ClO_4^-)$ 1145, 1112, 1082 cm^{-1}. ^1H NMR (DMSO-d_6): $\delta = 1.42$ (1H, s, broad, NH), 8.51 (1H, s), 8.49 (1H, s), 7.83 (1H, s), 3.0−3.4 (m, 4H, CH_2). Λ_M: 206 S mol^{-1} cm^2 in DMF. Mp: >300 °C.

$[Co(H_{1.5}L^6)](ClO_4)_{1.5}\cdot 4H_2O$ (6′). An aqueous solution of 0.1 M NaOH (7.5 mL, 0.75 mmol) was added to a solution of **6** (0.377 g, 0.5 mmol) in 30 mL of methanol. After the solution was stirred for 5 min at room temperature, it was filtered. The filtrate was allowed to stand for several days. The red-orange crystalline precipitate was collected by suction filtration, washed with a small volume of methanol, and dried in vacuo. Yield: 0.194 g (58%). Anal. Calcd for $[Co(H_{1.5}L^6)](ClO_4)_{1.5}\cdot 4H_2O$: C, 32.80; H, 4.66; N, 21.25. Found: C, 32.91; H, 4.51; N, 21.42. IR (KBr): $\nu_{C=N}$(imine) 1625, 1594 cm^{-1}; $\nu_{Cl-O}(ClO_4^-)$ 1143, 1121, 1059 cm^{-1}. Λ_M: 129 S mol^{-1} cm^2 in DMF. Mp: >280 °C.

$[Co(L^6)]\cdot 2.5H_2O$ (6″). A 3 equiv amounts of aqueous 0.1 M NaOH solution (1.5 mmol) was added to a solution of **6** (0.377 g, 0.5 mmol) in 50 mL of methanol. After the solution was stirred for 30 min in a water bath, it was filtered. The filtrate was allowed to stand for several days. The red-orange crystalline precipitate was collected by suction filtration, washed with a small volume of methanol, and dried in vacuo. Yield: 0.102 g (41%). Anal. Calcd for $[Co(L^6)]\cdot 2.5H_2O$: C, 44.91; H, 5.44; N, 29.10. Found: C, 44.81; H, 5.41; N, 29.12. IR (KBr): $\nu_{C=N}$(imine) 1597 cm^{-1}. Λ_M: insoluble in common organic solvents. Mp: >300 °C.

$[Co(H_{1.5}L^6)]Cl_{1.5}\cdot 4H_2O$ (6a′). To the ligand solution (1 mmol) was added a solution of *trans*-$[CoCl_2(py)_4]Cl$ (0.482 g, 1 mmol) in 20 mL of methanol. After being stirred for 1 h at room temperature, the solution was evaporated to dryness. The crude product was recrystallized from aqueous solution at pH = 3−4, adjusted by the addition of 0.1 M HCl. The red-orange crystals of the crude product $[Co(H_3L^6)]Cl_3$ (**6a**) were collected. A 1.5 equiv amount of triethylamine was added to a solution of the crude product **6a** in 20 mL of methanol. The solution was filtered, and the filtrate was allowed to stand for several days. Anal. Calcd for $[Co(H_{1.5}L^6)]Cl_{1.5}\cdot 4H_2O$: C, 38.36; H, 5.54; N, 24.85. Found: C, 38.57;

H, 5.35; N, 25.05. IR (KBr): $\nu_{C=N}$(imine), 1594 + shoulder cm^{-1}. Λ_M: 62 S mol^{-1} cm^2 in DMF. Mp: >300 °C.

[Co(H$_{1.5}$L^6)](NO$_3$)$_{1.5}$ (6b′). A solution of excess $NaNO_3$ in methanol was added to a solution of the crude product **6a** in 20 mL of methanol. The solution was allowed to stand overnight, and the orange crystals of [Co(H$_3$L^6)](NO$_3$)$_3$ (**6b**) that precipitated were collected. A 1.5 equiv amount of triethylamine was added to a solution of [Co(H$_3$L^6)](NO$_3$)$_3$ (**6b**) in methanol. The solution was filtered, and the filtrate was allowed to stand for several days. Anal. Calcd for [Co(H$_{1.5}$L^6)](NO$_3$)$_{1.5}$: C, 40.72; H, 4.27; N, 30.34. Found: C, 40.36; H, 4.22; N, 30.12. IR (KBr): $\nu_{C=N}$(imine), 1593 + shoulder cm^{-1}; ν_{N-O}(NO_3^-), 1381 cm^{-1}. Λ_M: 84 S mol^{-1} cm^2 in DMF. Mp: >300 °C. Preliminary cell dimensions: trigonal, $a = b = 12.59$ Å, $c = 18.38$ Å, $V = 2527.3$ Å^3.

Tris[2-(((2-methylimidazoyl-4-yl)methylidene)amino)ethyl]-amine H$_3$L^7. The ligand was prepared by a method similar to that for H$_3$L,[6] using 2-methyl-4-formylimidazole instead of 4-formylimidazole. The ligand solution was subsequently used for the synthesis of the Co(III) complex without isolation of the ligand.

[Co(H$_3$L^7)](ClO$_4$)$_3$·0.5H$_2$O (7). A method similar to the synthesis of **6** was adopted, yielding dark red crystals. Anal. Calcd for [Co(H$_3$L^7)](ClO$_4$)$_3$·0.5H$_2$O: C, 31.97; H, 3.96; N, 17.76. Found: C, 31.90; H, 4.01; N, 17.61. IR (KBr): $\nu_{C=N}$(imine), 1634 cm^{-1}; ν_{Cl-O}(ClO_4^-) 1145, 1117, 1082 cm^{-1}. Λ_M: 198 S mol^{-1} cm^2 in DMF. Mp: >300 °C.

[Co(H$_{1.5}$L^7)](ClO$_4$)$_{1.5}$ (7′). A method similar to the synthesis of **6′** was adopted, yielding red crystals. Anal. Calcd for [Co(H$_{1.5}$L^7)](ClO$_4$)$_{1.5}$: C, 40.09; H, 4.57; N, 22.26. Found: C, 40.02; H, 4.56; N, 22.21. IR (KBr): $\nu_{C=N}$(imine) 1635, 1609; ν_{Cl-O}(ClO_4^-) intense broad bands around 1083 cm^{-1}. Λ_M: 111 S mol^{-1} cm^2 in DMF. Mp: >300 °C.

[Co(L^7)]·3.5H$_2$O (7″). A method similar to the synthesis of **6″** was adopted, yielding orange crystals. Anal. Calcd for [Co(L^7)]·3.5H$_2$O: C, 46.58; H, 6.33; N, 25.87. Found: C, 46.79; H, 6.31; N, 25.63. IR (KBr): $\nu_{C=N}$(imine), 1596 cm^{-1}. Λ_M: 0.7 S mol^{-1} cm^2 in DMF. Mp: >300 °C.

Physical Measurements. Elemental analyses for C, H, and N were performed at the Elemental Analyses Service Center of Kyushu University. Infrared spectra were recorded using a Perkin-Elmer FT-IR Paragon 1000 spectrometer with KBr disks. Electrical conductivity measurements were carried out on a Horiba DS-14 conductometer in ca. 10^{-3} M *N*,*N*-dimethylformamide solutions. Circular dichroism spectra were measured using a JASCO J-720 spectropolarimeter in dimethyl sulfoxide.

Potentiometric pH Titrations. All titrations were carried out in a thermostat bath held at 25 °C under a 99.9995% N_2 atmosphere. Extrapure grade water with a resistance higher than 18.0 MΩ was used. The automatic buret Dosimat 665 was supplied by METROHM, Ltd. (Switzerland). The GS-5015c conjugated proton electrode and the IM-40S potentiometer were supplied by TOA Co., Ltd. (Japan). The standard electrode potential ($E°$) was first determined using Gran's plot method.[28] An 80 mL solution of 0.15 M ionic strength containing 0.055 mmol of the metal complex and sodium chloride was titrated with a solution containing 0.05 M NaOH and 0.10 M NaCl. Immediately after the forward titration, the resulting solution was back-titrated with a solution containing 0.05 M HCl and 0.10 M NaCl. All titrations and potential measurements were PC-controlled. The electrode potentials were converted to a proton concentration scale ($-\log [H^+] = (E°(mV) - E(mV))/59.15$), and the proton association degree, n, was calculated using Bjerrum's method for the forward and reverse titrations.[31]

pH-Dependent Electronic Spectra. The pH-dependent electronic spectral changes were recorded at room temperature on sequential addition of 0.10 M NaOH and HCl aqueous solutions for the forward and reverse titrations, respectively. An aqueous solution of the protonated complex (0.24 mmol of the complex in 80 mL of water) was prepared. A spectrum was recorded after each 0.40 mL addition of a 0.10 M NaOH solution, until 3 equiv of NaOH was added. Immediately after, the electronic spectra were recorded for the reverse titration, following each 0.40 mL addition of a 0.10 M HCl solution to the solution resulting from the forward titration. The spectra were corrected for the volume variation due to the addition of the NaOH and HCl solutions.

X-ray Data Collection, Reduction, and Structure Determination. Single crystals were mounted on a glass fiber and coated with epoxy resin. All crystallographic measurements were carried out using a Rigaku AFC-7R diffractometer with graphite-monochromated Mo Kα radiation ($\lambda = 0.710\ 69$ Å) and a 12 kW rotating anode generator. The data were collected at a temperature of 20 ± 1 °C using the $\omega-2\theta$ scan technique to a maximum 2θ value of 50.0° with a scan speed of 8.0−16.0°/min (in omega). The weak reflections ($I < 10.0\sigma(I)$) were rescanned (maximum of five scans), and the counts were accumulated to ensure good counting statistics. The intensities of three standard reflections were measured after every 150 reflections. Over the course of the data collection, the standard reflections were monitored, and decay corrections were applied through a polynomial expression. An empirical absorption correction based on the azimuthal scans of several reflections was applied. The data were also corrected for Lorentz and polarization effects.

The structures were solved using the DIRDIF92(PATTY) package and expanded using Fourier techniques.[34,35] The non-hydrogen atoms, except for the disordered atoms, were anisotropically refined. Hydrogen atoms at their ideal calculated positions were included in the structure factor calculations but not refined, except for **7′**. Full-matrix least-squares refinements ($I > 2.00\sigma(I)$) were employed, where the unweighted and weighted agreement factors of $R = \sum||F_o| - |F_c||/\sum|F_o|$ and $R_w = [\sum w(|F_o| - |F_c|)^2/\sum w|F_o|^2]^{1/2}$ were used. In the least-squares refinement for the crystals with the noncentrosymmetric space groups, the Flack parameter defined as $|F| = (1 - x)|F(+)| + x|F(-)|$ was refined to determine the absolute configuration.[36]

Neutral atomic scattering factors were taken from Cromer and Waber.[37] Anomalous dispersion effects were included in F_c; the values $\Delta f'$ and $\Delta f''$ used were those of Creagh and McAuley.[38] The values for the mass attenuation coefficients were those of Creagh and Hubbel.[39] All calculations were performed using the teXsan crystallographic software package from Molecular Structure Corporation.[40] Crystal data and details of the structure determination for **6**, **6′**, **6″**, and **6a′** and **7**, **7′**, and **7″** are summarized in Tables 3 and 4, respectively.

Acknowledgment. This work was supported by Grants-in-Aid for Scientific Research in Priority Areas (No. 11136236, "Metal-Assembled Complexes") from the Ministry of Education, Science, and Culture of Japan. Financial support from the Okayama Foundation for Science and Technology is gratefully acknowledged.

Supporting Information Available: X-ray crystallographic files for the structure determinations of [Co(H$_3$L^6)](ClO$_4$)$_3$·H$_2$O (**6**), [Co(H$_{1.5}$L)](ClO$_4$)$_{1.5}$·4H$_2$O (**6′**), [Co(L^6)]·2.5H$_2$O (**6″**), [Co(H$_{1.5}$L^6)]Cl$_{1.5}$·4H$_2$O (**6a′**), [Co(H$_3$L^7)](ClO$_4$)$_3$·0.5H$_2$O (**7**), [Co(H$_{1.5}$L^7)](ClO$_4$)$_{1.5}$ (**7′**), and [Co(L^7)]·3.5H$_2$O (**7″**) (CIF). This material is available free of charge via the Internet at http://pubs.acs.org.

JA0123960

(34) Beurskens, P. T.; Admiraal, G.; Beurskens, G.; Bosman, W. P.; Garcia-Granda, S.; Gould, R. O.; Smits, J. M. M.; Smikalla, C. *DIRDIF92*: *The DIRDIF Program System, Technical Report of the Crystallography Laboratory*; University of Nijmegen: The Netherlands, 1992.
(35) Fan Hai-Fu. *SAPI91*: *Structure Analysis Programs with Intelligent Control*; Rigaku Corp.: Tokyo, Japan, 1991.
(36) Flack, H. D. *Acta Crystallogr., Sect. A* **1993**, *39*, 876−881.
(37) Cromer, D. T.; Waber, J. T. *International Tables for X-ray Crystallography*; The Kynoch Press: Birmingham, England, 1974; Vol. IV, Table 2.2A.
(38) Creagh, D. C.; McAuley, W. J. In *International Tables for Crystallography*; Wilson, A. J. C., Ed.; Kluwer Academic Publishers: Boston, MA, 1992; Vol. C, Table 4.2.6.8, pp 219−222.
(39) Creagh, D. C.; Hubbel, J. H. In *International Tables for Crystallography*; Wilson, A. J. C., Ed.; Kluwer Academic Publishers: Boston, MA, 1992; Vol. C, Table 4.2.4.3, pp 200−206.
(40) *teXsan*: *Crystal Structure Analysis Package*; Molecular Structure Corporation: The Woodlands, TX, 1985 and 1992, teXan for Windows Version 1.04.